

# MASSES AND DEFORMATIONS OF NEUTRON-RICH NUCLEI

J. RAYFORD NIX and PETER MÖLLER

*Theoretical Division, Los Alamos National Laboratory*

*Los Alamos, New Mexico 87545, USA*

*E-mail: nix@t2nix.lanl.gov and moller@moller.lanl.gov*

We have calculated the masses, deformations, and other properties of 8979 nuclei ranging from  $^{16}\text{O}$  to  $^{339}136$  and extending from the proton drip line to the neutron drip line on the basis of the 1992 version of the finite-range droplet model. The predicted quantities include the ground-state mass, deformation, microscopic correction, odd-proton and odd-neutron spins and parities, proton and neutron pairing gaps, binding energy, one- and two-neutron separation energies, quantities related to  $\beta$ -delayed one- and two-neutron emission probabilities,  $\beta$ -decay energy release and half-life with respect to Gamow-Teller decay, one- and two-proton separation energies, and  $\alpha$ -decay energy release and half-life. For 1654 nuclei heavier than  $^{16}\text{O}$  whose masses were known experimentally in 1989 and which were included in the adjustment of model constants, the theoretical error is 0.669 MeV. For 371 additional nuclei heavier than  $^{16}\text{O}$  whose masses have been measured between 1989 and 1996 and which were not used in the adjustment of the model constants, the theoretical error is 0.570 MeV.

## 1 Introduction

The accurate calculation of the ground-state mass and deformation of a nucleus far from stability, such as one of the neutron-rich nuclei considered in this conference, remains one of the most fundamental challenges of nuclear theory. Toward this goal, two major approaches—which also allow the simultaneous calculation of a wide variety of other nuclear properties—have been developed (along with numerous semi-empirical formulas for masses alone).

At the most fundamental level, fully selfconsistent microscopic theories, starting with an underlying nucleon-nucleon interaction, have seen progress in both the nonrelativistic Hartree-Fock approximation and more recently the relativistic mean-field approximation. Although microscopic theories offer great promise for the future, their current accuracies are typically a few MeV, which is insufficient for most practical applications. At the next level of fundamentality, the macroscopic-microscopic method—where the smooth trends are obtained from a macroscopic model and the local fluctuations from a microscopic model—has been used in several recent global calculations that are useful for a broad range of applications.

We will concentrate here on the 1992 version of the finite-range droplet model,<sup>1,2</sup> with particular emphasis on its reliability for extrapolations to new regions of nuclei, but will also briefly discuss two other models of this type.<sup>3,4</sup>

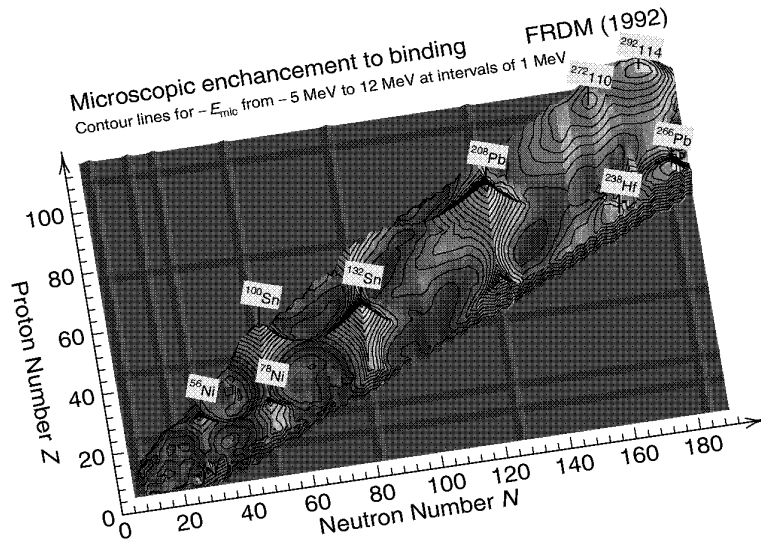


Figure 1: Calculated additional binding energy of even-even nuclei relative to the macroscopic energy of spherical nuclei, illustrating the crucial role of microscopic corrections.

## 2 Finite-Range Droplet Model

In the finite-range droplet model, which takes its name from the macroscopic model that is used, the microscopic shell and pairing corrections are calculated from a realistic, diffuse-surface, folded-Yukawa single-particle potential by use of Strutinsky's method.<sup>5</sup> In 1992 we made a new adjustment of the constants of an improved version of this model to 28 fission-barrier heights and to 1654 nuclei with  $N, Z \geq 8$  ranging from  $^{16}\text{O}$  to  $^{263}106$  whose masses were known experimentally in 1989.<sup>6</sup> The resulting microscopic enhancement to binding for even-even nuclei throughout the periodic system is shown in Fig. 1.

This model has been used to calculate the ground-state mass, deformation, microscopic correction, odd-proton and odd-neutron spins and parities, proton and neutron pairing gaps, binding energy, one- and two-neutron separation energies, quantities related to  $\beta$ -delayed one- and two-neutron emission probabilities,  $\beta$ -decay energy release and half-life with respect to Gamow-Teller decay, one- and two-proton separation energies, and  $\alpha$ -decay energy release and half-life for 8979 nuclei with  $N, Z \geq 8$  ranging from  $^{16}\text{O}$  to  $^{339}136$  and extending from the proton drip line to the neutron drip line.<sup>1,2</sup> These tabulated quantities are available electronically on the World Wide Web at the Uniform Resource Locator <http://t2.lanl.gov/publications/publications.html>.

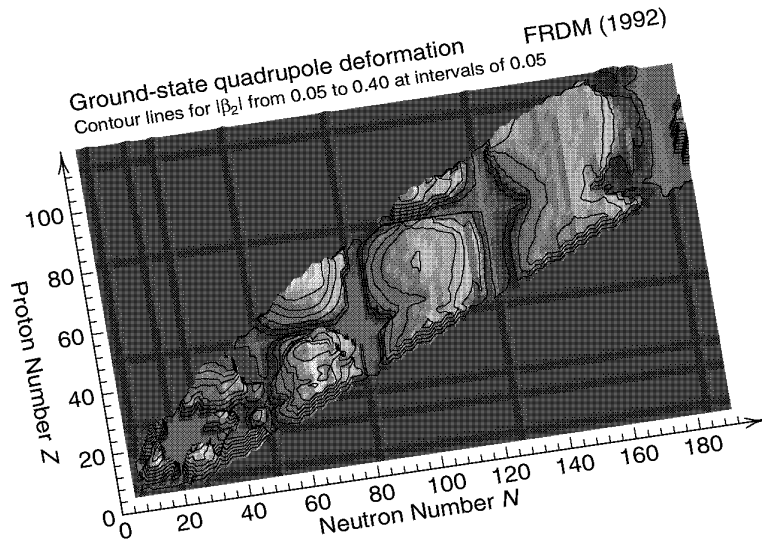


Figure 2: Calculated quadrupole deformations of even-even nuclei, illustrating the transitions from spherical to deformed nuclei as one moves away from magic numbers.

### 3 Ground-State Deformations

In our calculations, we specify a general nuclear shape in terms of deviations from a spheroidal shape by use of Nilsson's  $\epsilon$  parameterization.<sup>7</sup> The ground-state shape is determined by initially minimizing the nuclear potential energy of deformation with respect to the two symmetric shape coordinates  $\epsilon_2$  and  $\epsilon_4$ . During this minimization, we include a prescribed smooth dependence of the higher symmetric deformation  $\epsilon_6$  on the two independent coordinates  $\epsilon_2$  and  $\epsilon_4$ . This dependence is determined by minimizing the macroscopic potential energy of  $^{240}\text{Pu}$  with respect to  $\epsilon_6$  for fixed values of  $\epsilon_2$  and  $\epsilon_4$ . We then vary separately  $\epsilon_6$  and the mass-asymmetric, or octupole, deformation  $\epsilon_3$ , with  $\epsilon_2$  and  $\epsilon_4$  held fixed at their previously determined values, to calculate any additional lowering in energy from these two degrees of freedom.

For presentation purposes, it is sometimes more convenient to express the nuclear ground-state shape in terms of the  $\beta$  parameterization, where the shape coordinates represent the coefficients in an expansion of the radius vector to the nuclear surface in a series of spherical harmonics. Figures 2 and 3 show our calculated quadrupole and hexadecapole deformations, respectively, in terms of  $\beta_2$  and  $\beta_4$ , which are determined by transforming our calculated shapes from the  $\epsilon$  parameterization.

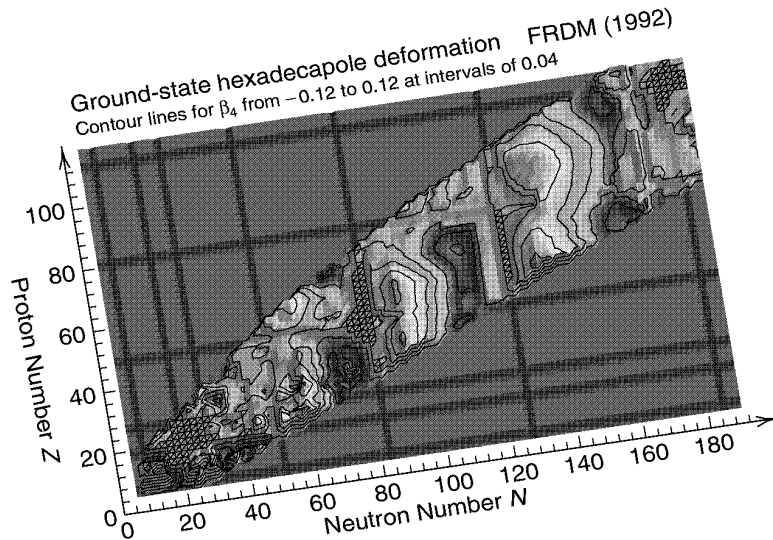


Figure 3: Calculated hexadecapole deformations of even-even nuclei, illustrating the transitions from bulging to indented equatorial regions as one moves from smaller to larger magic numbers.

The inclusion of the  $\epsilon_6$  and  $\epsilon_3$  shape degrees of freedom is crucial for the isolation of such physical effects as the Coulomb redistribution energy, which arises from a central density depression.<sup>8</sup> As illustrated in Fig. 4, an independent variation of the symmetric deformation  $\epsilon_6$  is important for several regions of nuclei. For even-even nuclei, the maximum reduction in energy relative to that for a prescribed smooth  $\epsilon_6$  dependence is 1.28 MeV and occurs for  $^{252}\text{Fm}$ . As illustrated in Fig. 5, the mass-asymmetric deformation  $\epsilon_3$  is important for nuclei in a few isolated regions. For even-even nuclei, the maximum reduction in energy relative to that for a symmetric shape is 1.29 MeV and occurs for the neutron-rich nucleus  $^{194}\text{Gd}$ . For even-even nuclei close to the valley of  $\beta$ -stability, the maximum reduction in energy relative to that for a symmetric shape is 1.20 MeV and occurs for  $^{222}\text{Ra}$ .

#### 4 Reliability for Extrapolations to New Regions of Nuclei

For the original 1654 nuclei included in the adjustment, the theoretical error, determined by use of the maximum-likelihood method with no contributions from experimental errors,<sup>1,2</sup> is 0.669 MeV. Although some large systematic errors exist for light nuclei, they decrease significantly for heavier nuclei.

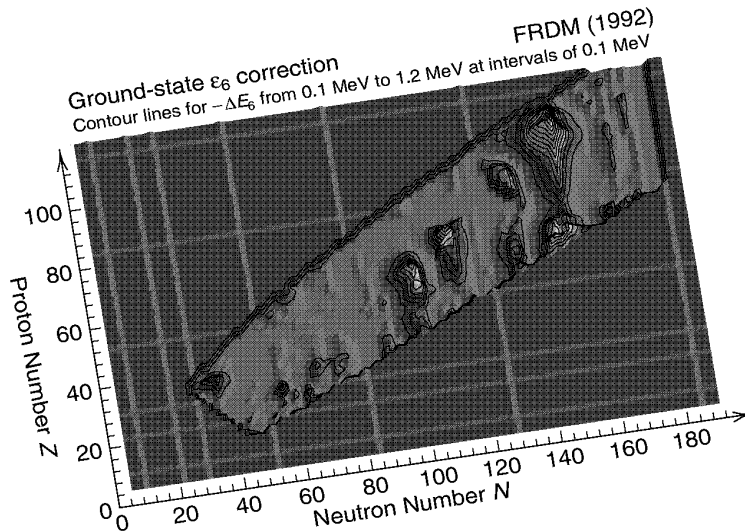


Figure 4: Calculated reduction in energy of even-even nuclei arising from an independent variation in  $\epsilon_6$ , relative to that for shapes with a prescribed smooth  $\epsilon_6$  dependence. Note that the sign of the  $\epsilon_6$  correction is reversed in this plot for clarity of display.

Between 1989 and 1996, the masses of 371 additional nuclei heavier than  $^{16}\text{O}$  have been measured,<sup>9–11</sup> which provides an ideal opportunity to test the ability of mass models to extrapolate to new regions of nuclei whose masses were not included in the original adjustment. Figure 6 shows as a function of the number of neutrons from  $\beta$ -stability the individual deviations between these newly measured masses and those predicted by the 1992 finite-range droplet model. The new nuclei fall into three categories, with the first category corresponding to 273 nuclei lying on both sides of the valley of  $\beta$ -stability.<sup>9</sup> The second category corresponds to 91 proton-rich nuclei produced by fragmentation of  $^{209}\text{Bi}$  projectiles incident on a thick Be target in the experimental storage ring (ESR) at the Gesellschaft für Schwerionenforschung (GSI) in Darmstadt, Germany.<sup>10</sup> The third category corresponds to seven proton-rich superheavy nuclei discovered in the separator for heavy-ion reaction products (SHIP) at GSI whose masses are estimated by adding the highest  $\alpha$ -decay energy release at each step in the decay chain to known masses.<sup>11</sup> This procedure could seriously overestimate the experimental masses of some of the heavier nuclei because different energy releases have been observed in some cases.<sup>11</sup> To account for this uncertainty, we have assigned a mass error of 0.5 MeV for each of these seven nuclei. Also, to account for errors of unknown origin, we

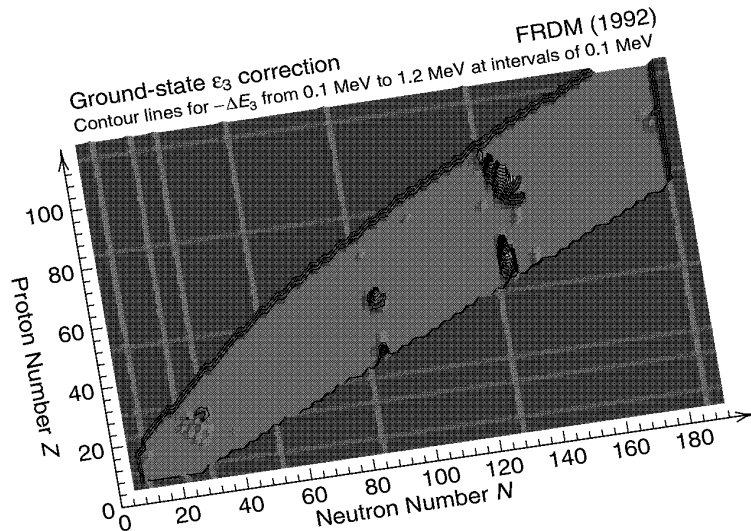


Figure 5: Calculated reduction in energy of even-even nuclei arising from the inclusion of  $\epsilon_3$  deformations, relative to that for symmetric shapes. Note that the sign of the  $\epsilon_3$  correction is reversed in this plot for clarity of display.

have included an additional 0.076 MeV contribution<sup>12</sup> to the mass errors for each of the 91 nuclei in the second category. The theoretical error of the 1992 finite-range droplet model [FRDM (1992)] for all of the 371 newly measured masses is 0.570 MeV. The reduction in error arises partly because most of the new nuclei are located in the heavy region, where the model is more accurate.

Analogous deviations occur for version 1 of the 1992 extended-Thomas-Fermi Strutinsky-integral [ETFSI-1 (1992)] model of Aboussir, Pearson, Dutta, and Tondeur.<sup>3</sup> In this model, the macroscopic energy is calculated for a Skyrme-like nucleon-nucleon interaction by use of an extended Thomas-Fermi approximation. The shell correction is calculated from single-particle levels corresponding to this same interaction by use of a Strutinsky-integral method, and the pairing correction is calculated for a  $\delta$ -function pairing interaction by use of the conventional BCS approximation. The constants of the model were determined by adjustments to the ground-state masses of 1492 nuclei with mass number  $A \geq 36$ , which excludes the troublesome region from  $^{16}\text{O}$  to mass number  $A = 35$ . The theoretical error corresponding to 1540 nuclei whose masses were known experimentally<sup>6</sup> at the time of the original adjustment is 0.733 MeV. The theoretical error for 366 newly measured masses<sup>9-11</sup> for nuclei with  $A \geq 36$  is 0.739 MeV.

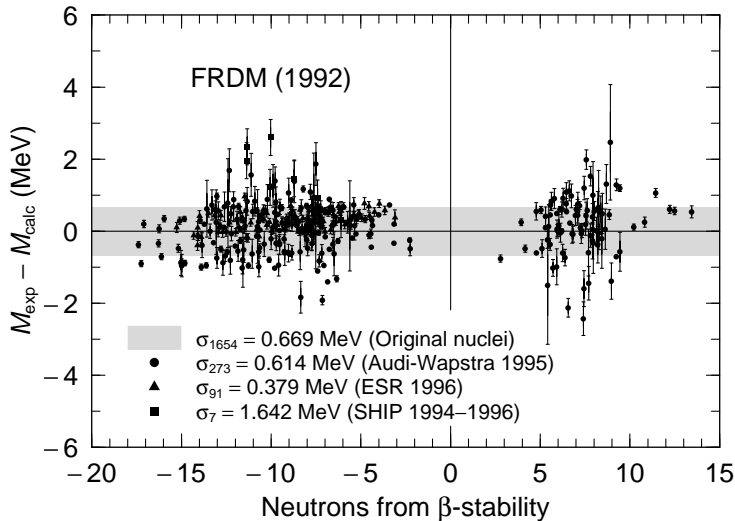


Figure 6: Deviations between experimental and calculated masses for 371 new nuclei whose masses were not included in the 1992 adjustment of the finite-range droplet model.<sup>1,2</sup>

Similar results hold for the 1994 Thomas-Fermi [TF (1994)] model of Myers and Swiatecki.<sup>4</sup> In this model, the macroscopic energy is calculated for a generalized Seyler-Blanchard nucleon-nucleon interaction by use of the original Thomas-Fermi approximation. For  $N, Z \geq 30$  the shell and pairing corrections were taken from the 1992 finite-range droplet model, and for  $N, Z \leq 29$  a semi-empirical expression was used. The constants of the model were determined by adjustments to the ground-state masses of the same 1654 nuclei with  $N, Z \geq 8$  ranging from  $^{16}\text{O}$  to  $^{263}106$  whose masses were known experimentally in 1989 that were used in the 1992 finite-range droplet model. The theoretical error corresponding to these 1654 nuclei is 0.640 MeV. The reduced theoretical error relative to that in the 1992 finite-range droplet model arises primarily from the use of semi-empirical microscopic corrections in the extended troublesome region  $N, Z \leq 29$  rather than microscopic corrections calculated more fundamentally. The theoretical error for 371 newly measured masses<sup>9-11</sup> is 0.620 MeV.

As summarized in Table 1, the theoretical error for the newly measured masses relative to that for the original masses to which the model constants were adjusted *decreases* by 15% for the FRDM (1992), increases by 1% for the ETFSI-1 (1992) model, and *decreases* by 3% for the TF (1994) model. These macroscopic-microscopic mass models can therefore be extrapolated to new regions of nuclei with differing amounts of confidence.

Table 1: Extrapolateability of Three Mass Models to New Regions of Nuclei.

| Model          | Original nuclei  |             | New nuclei       |             |             |
|----------------|------------------|-------------|------------------|-------------|-------------|
|                | $N_{\text{nuc}}$ | Error (MeV) | $N_{\text{nuc}}$ | Error (MeV) | Error ratio |
| FRDM (1992)    | 1654             | 0.669       | 371              | 0.570       | 0.85        |
| ETFSI-1 (1992) | 1540             | 0.733       | 366              | 0.739       | 1.01        |
| TF (1994)      | 1654             | 0.640       | 371              | 0.620       | 0.97        |

## 5 Rock of Metastable Superheavy Nuclei

The heaviest nucleus known to man,  $^{277}112$ , was discovered<sup>13</sup> in February 1996 at the GSI by use of the gentle fusion reaction  $^{70}\text{Zn} + ^{208}\text{Pb} \rightarrow ^1_0\text{n} + ^{277}112$ . It is the latest in a series of about 10 recently discovered nuclei<sup>13-17</sup> lying on a rock of deformed metastable superheavy nuclei predicted to exist<sup>1,2,18-20</sup> near the deformed proton magic number at 110 and deformed neutron magic number at 162. These 10 superheavy nuclei are shown in Fig. 7 as tiny deformed three-dimensional objects. Most of the metastable superheavy nuclei that have been discovered live for only about a thousandth of a second, after which they generally decay by emitting a series of alpha particles. However, the decay products of the most recently discovered nucleus  $^{277}112$  show for the first time that nuclei at the center of the predicted rock of stability live longer than 10 seconds.

We have used the macroscopic-microscopic method recently to calculate the fusion barrier for several reactions leading to deformed superheavy nuclei.<sup>21</sup> For the reaction  $^{70}\text{Zn} + ^{208}\text{Pb} \rightarrow ^1_0\text{n} + ^{277}112$ , the microscopic shell and pairing corrections associated primarily with the doubly magic  $^{208}\text{Pb}$  target nucleus lower the total potential energy at the touching configuration by about 12 MeV relative to the macroscopic energy. These shell and pairing corrections persist from the touching configuration inward to a position only slightly more deformed than the ground-state shape. The resulting maximum in the fusion barrier is about 2 MeV lower than the center-of-mass energy that was used in the GSI experiment that produced  $^{277}112$ .

One possibility to reach the island of spherical superheavy nuclei near  $^{290}110$  that is predicted to lie beyond our present horizon involves the use of prolately deformed targets and projectiles that also possess large negative hexadecapole moments, which leads to large indented equatorial regions.<sup>22</sup>



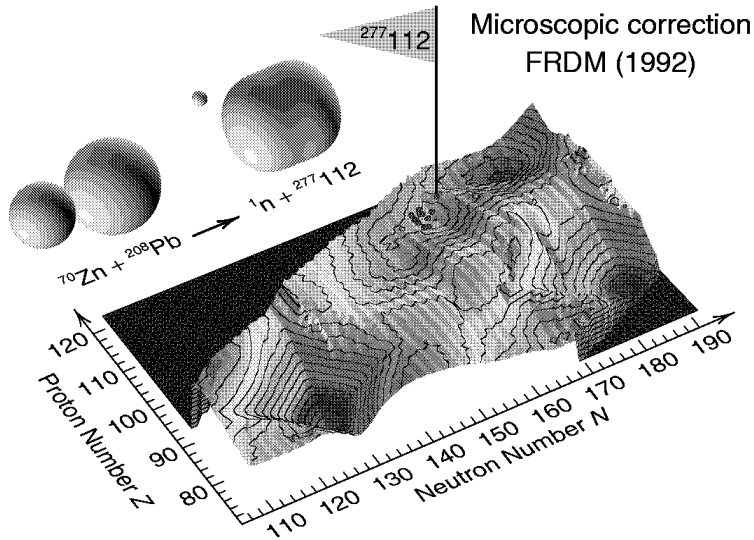


Figure 7: Ten recently discovered superheavy nuclei,<sup>13–17</sup> superimposed on a theoretical calculation<sup>1,2</sup> of the microscopic corrections to the ground-state masses of nuclei extending from the vicinity of lead to heavy and superheavy nuclei. The heaviest nucleus, whose location on the diagram is indicated by the flag, was produced through a gentle reaction between spherical  $^{70}\text{Zn}$  and  $^{208}\text{Pb}$  nuclei in which a single neutron was emitted.<sup>13</sup>

## 6 Summary and Conclusion

The FRDM (1992) and two other macroscopic-microscopic models have been used recently to calculate the ground-state masses and deformations of nuclei throughout our known chart and beyond, and the FRDM (1992) has also been used to simultaneously calculate a wide variety of other nuclear properties. These models are useful for extrapolating to new regions of nuclei whose masses were not included in the original adjustment. Macroscopic-microscopic models have also correctly predicted the existence and location of a rock of deformed metastable superheavy nuclei near  $^{272}110$  that has recently been discovered. Nuclear ground-state masses and deformations will continue to provide an invaluable testing ground for nuclear many-body theories. The future challenge is for fully selfconsistent microscopic theories to predict these quantities with comparable or greater accuracy.

## Acknowledgments

This work was supported by the U. S. Department of Energy.

## References

1. P. Möller, J. R. Nix, W. D. Myers, and W. J. Swiatecki, *Atomic Data Nucl. Data Tables* **59**, 185 (1995).
2. P. Möller, J. R. Nix, and K. L. Kratz, *Atomic Data Nucl. Data Tables* **66**, 131 (1997).
3. Y. Aboussir, J. M. Pearson, A. K. Dutta, and F. Tondeur, *Atomic Data Nucl. Data Tables* **61**, 127 (1995).
4. W. D. Myers and W. J. Swiatecki, *Nucl. Phys. A* **601**, 141 (1996).
5. V. M. Strutinsky, *Nucl. Phys. A* **122**, 1 (1968).
6. G. Audi, Midstream Atomic Mass Evaluation, private communication (1989), with four revisions.
7. S. G. Nilsson, K. Dan. Vidensk. Selsk. Mat. Fys. Medd. **29**, 16 (1955).
8. P. Möller, J. R. Nix, W. D. Myers, and W. J. Swiatecki, *Nucl. Phys. A* **536**, 61 (1992).
9. G. Audi and A. H. Wapstra, *Nucl. Phys. A* **595**, 409 (1995).
10. T. F. Kerscher, Ph. D. Thesis, Fakultät für Physik, Ludwig-Maximilians-Universität München (1996).
11. S. Hofmann, *Z. Phys. A* **358**, 125 (1997).
12. Yu. Norikov, private communication (1996).
13. S. Hofmann et al., *Z. Phys. A* **354**, 229 (1996).
14. S. Hofmann et al., *Z. Phys. A* **350**, 277 (1995).
15. S. Hofmann et al., *Z. Phys. A* **350**, 281 (1995).
16. Yu. A. Lazarev et al., *Phys. Rev. Lett.* **73**, 624 (1994).
17. Yu. Ts. Oganessian, *Nucl. Phys. A* **583**, 823c (1995).
18. P. Möller and J. R. Nix, *Atomic Data Nucl. Data Tables* **26**, 165 (1981).
19. R. Bengtsson, P. Möller, J. R. Nix, and Jing-ye Zhang, *Phys. Scr.* **29**, 402 (1984).
20. Z. Patyk and A. Sobczewski, *Phys. Lett. B* **256**, 307 (1991).
21. P. Möller, J. R. Nix, P. Armbruster, S. Hofmann, and G. Münzenberg, *Z. Phys. A*, in press.
22. A. Iwamoto, P. Möller, J. R. Nix, and H. Sagawa, *Nucl. Phys. A* **596**, 329 (1996).